AD-A089 447 FOREIGN TECHNOLOGY DIV WRIGHT-PATTERSON AFB OH F/G 20/5
A THERMODYNAMIC MODEL FOR CO2 LASERS,(U)
AUG 80 D C DUMITRAS
UNCLASSIFIED FTD-ID(RS)T-1023-80 NL

END
DATE FILMED
10-80
DTIC

FTD-ID(RS)T-1023-80

FOREIGN TECHNOLOGY DIVISION

A THERMODYNAMIC MODEL FOR CO_2 LASERS

by

D. C. Dumitras

Approved for public release;
distribution unlimited.

EDITED TRANSLATION

(14) FTD-ID(RS)T-1023-80 (11) 8 August 1980

MICROFICHE NR: FTD-80-C-000937

A THERMODYNAMIC MODEL FOR CO_2 LASERS

By: (10) D. C. Dumitras

(13) 31

English pages: 28

Source: (21) Studii si Cercetari de Fizica, Vol. 30, Nr. 7, 1978, pp. 671-694

Country of origin: Romania

Translated by: SCITRAN
F33657-78-D-0619

Requester: FTD/TQTD

A

PREPARED BY:

TRANSLATION DIVISION
FOREIGN TECHNOLOGY DIVISION
WP-AFB, OHIO.

111600

A THERMODYNAMIC MODEL FOR CO_2 LASERS [1)]

by D. C. Dumitras

Central Physics Institute, Bucharest P.O. Box 5206
Inst. for Physics and Technology of Radiation Equipment

1. Introduction

In ord r to optimize the functioning of a CO_2 laser with wave guide, it is important to be able to calculate the dependence of the small signal gain as a function of a number of parameters such as: gas mixture, total pressure, discharge current, tube diameter, temperature of the cooling jacket, etc. If the kinetic temperature and the population of the laser levels are known as a function of these parameters, the gain equations are uniquely determined. The complexity of the energy level diagram for the CO_2 molecule, the large number of rates of collisional excitation and relaxation and their dependence on temperature, diffusion and relaxation processes through collisions with the walls of the enclosure, the great number of additives that participate in the population inversion, add to the difficulty of the analytical treatment of the laser effect and of the gain, saturation and oscillation bandwidth.

Since its inception, a number of models were proposed based on the rate equations relating the vibrational modes of the CO_2 and N_2 molecules. Thus, Moore et al [1] have divided the energy levels in three groups (each characterized by a single vibrational temperature), and solved the system of equations for the continuous wave regime. A comparison with experiment shows that this is a good simplification. Previous works considered separately the vibrational levels of nitrogen [2], [3], and 4 or 5 groups including also the

[1] Received on December 19, 1977

vibrational levels of Co[4].

The new elements in this work are: small tube diameters, high pressures and current densities characteristic to the wave guide lasers. These differences imply faster excitation and relaxation rates and also collisional widening of emission lines. The most recent determinations of the excitation and relaxation rates and their temperature dependence are utilized. This data was not available when [1] - [4] were published.

The main limitation of works dealing with thermodynamic models for CO_2 lasers are using calculated excitation and relaxation rates [2-5], which can differ appreciably from the measured ones; the gas temperature is determined from the wrong relationship [2-5];[1] neglects relaxation through diffusion and collision at the walls of the enclosure and is limited to a 3 level system; none of these works take into account the gas pressure dependence of the diffusional relaxation rate, and neglect the losses inherent when guiding radiation through small diameter tubes; [5] is limited to a fixed excitation rate and only one diameter of the discharge tube and does not take into account the saturation processes. Some recent attempts [63], [7] eliminate some of these problems but the system of equations used is still simplistic (3 level system).

The model presented here is used for lasers with wave guide. It can be used also for other CO_2 lasers with axial discharge and gas flow. For lasers without gas flow, the modifications of the rate equations are due to the kinetic temperature of the gas and eventual gaseous components which participate in the inversion in the CO_2 molecule (especially the carbon monoxide).

2. Physical Model

The lower vibrational energy levels for the CO_2 and N_2 system are shown in figure 1.

These levels are divided into four groups: group 0, including the fundamental levels (unexcited)of the CO_2 and N_2 molecules, with populations N_o and N_3^0 respectively; group 1, including the CO_2 molecules excited in the modes of symmetric elongation and deformation, with population N_1; group 2, CO_2 molecules with asymmetric elongation modes excited, population N_2; group 3, containing nitrogen molecules with one or more of the vibrational levels excited and population N_3. The total densities of CO_2 and nitrogen molecules are N_t and respectively N_{3t}.

Dividing the system CO_2 and N_2 in four groups seems justified by the rapid relaxation of the vibrational energy within each group, at a rate much larger than that of exchange of energy between groups. Thus CO_2 molecules in state 00°2 relax to state 00°1 at a rate larger than 5×10^6 s^{-1} $torr^{-1}$ [8], and the nitrogen molecules relax from the upper levels to state $v = 1$ in approximately 1μs [9]. Also the relaxation of the vibrational energy between levels in group 1 is rapid, it is thus possible to characterize the whole group by a single vibrational temperature. Groups 1-3 are excited through electronic collision with rates R_1 - R_3 and relax through diffusion and collisions with the walls of the enclosure with rates k_{1p} - k_{3p}. Group 1 is excited and relaxes collisionally with rates k_{10} and k_{01} respectively, and group 3 relaxes through electronic collisions at a rate k_{3e}. Vibrational energy is exchanged between groups 3 and 2 through a rapid V-V transfer, characterized by a rate k_{32} and the inverse rate k_{23}, and between groups 2 and 1 through collisions with molecules and atoms (rates k_{21} and k_{12}), collisions with discharge electrons (rate k_{2e}), through induced emission (rate W_{21}) and induced absorption (rate W_{12}). The inverse rate k_{23} between groups 2 and 3 is taken to be equal to the direct rate k_{32}. Rate k_{30} (due to collisions with molecules, atoms and electrons) is neglected, because such a collision is much more likely to relax a CO_2 molecule from

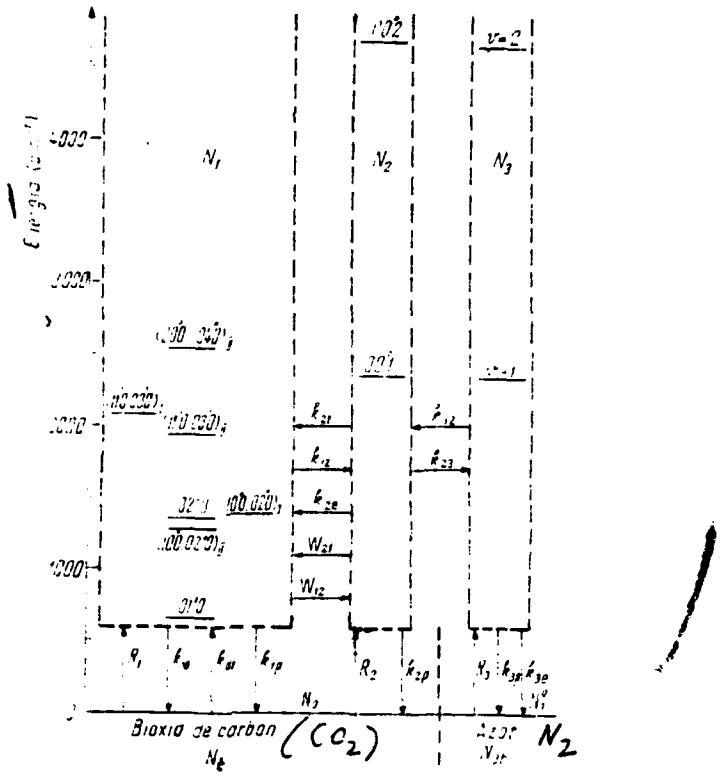

Figure 1. Diagram of lower vibrational energy levels for the CO_2 and N_2 system, grouped for the 4 level approximation.[2]

1 - energy;

state 00°1 to one of the states in group 1, rather than the fundamental level [9]. We assume also that the degree of dissociation of the CO_2 molecule is small (justified for the case of lasers with gas circulation).

2.1. Kinetic Temperature of the Gas

To calculate the gas temperature in the discharge one needs to solve the Fourier heat equation for the continuous wave generation regime

$$\nabla^2 T + q/\lambda_{\text{газ}} = 0, \tag{1}$$

where T is the gas temperature in K, g is the rate of change

of the heat due to sources and radiators expressed in Wm^{-3}, and λ_{mix} is the thermal conductivity of the gas mixture in $WK^{-1}m^{-1}$.

The source of heat is that part of the electron energy which is transferred to the translational energy of the molecules. Thus the radial distribution of the heat source is the same as the radial distribution of the electrons in the discharge.

From the theory of the positive column the radial distribution of the electron density is a zero order Bessel function, if the distribution is not affected by the strong radial temperature gradient

$$q = q_0 J_0 (2{,}405\ r/a). \tag{2}$$

Solving the heat equation with this q in cylindrical coordinates with boundary condition $T(a) = T_p$, for a cylinder of radius a and length L (length of discharge), one obtains

$$T - T_p = \frac{q}{\lambda_{mix}} \left(\frac{a}{2{,}405} \right)^2 J_0 (2{,}405\ r/a). \tag{3}$$

If we also consider the temperature gradient in the wall of the discharge tube (exterior radius a') then [7]

$$T = T_p + q_0 a^2 \left[\frac{0{,}1729}{\lambda_{mix}} + \frac{1}{2\lambda_p} \ln \left(\frac{a'}{a} \right) \right] J_0 (2{,}405\ r/a), \tag{4}$$

where λ_p is the thermal conductivity of the wall material. In the center of the tube (r=0) the gas temperature can be calculated from

$$T = T_p + q_0 a^2 \left[\frac{0{,}1729}{\lambda_{mix}} + \frac{1}{2\lambda_p} \ln \left(\frac{a'}{a} \right) \right]. \tag{5}$$

The total amount of heat which increases the translational energy of the molecules per unit time, Q, is obtained by integrating the source q over the volume

$$Q = \int_V \eta_0 J_0(2{,}405\ r/a)\, dV = 1{,}3582\ \eta_0 L a^2. \qquad (6)$$

Thus

$$T = T_p + \frac{Q}{L}\left[\frac{0{,}1274}{\lambda_{min}} + \frac{0{,}3686}{\lambda_p}\ln\left(\frac{a'}{a}\right)\right]. \qquad (7)$$

(Works [2] - [5] have used this formula, but the proportionality coefficient for $T - T_p$ was 2.4 times smaller).

In calculating the temperature of the gas mixture in the center of the tube, one has to take into account that not all the input power is turned into heat: part is turned into laser power; part to excite the molecules which in turn through diffusion and collisions lose it to the walls; and, in the case of lasers with gas circulation, part of the excited molecules leave the discharge zone, before their energy is turned into heat. Because of these, equations (5), (7) have to be adjusted by introducing a conversion coefficient η

$$T - T_p = \eta^* a^2 \eta_0 \left[\frac{0{,}1729}{\lambda_{min}} + \frac{1}{2\lambda_p}\ln\left(\frac{a'}{a}\right)\right], \qquad (8)$$

$$T - T_p = \eta^{**} \frac{Q}{L}\left[\frac{0{,}1274}{\lambda_{min}} + \frac{0{,}3686}{\lambda_p}\ln\left(\frac{a'}{a}\right)\right]. \qquad (9)$$

For closed CO_2 lasers, η^{**} varies between 0.5 and 0.8 [10], and for those with gas circulation between 0.05 and 0.3.

One can see from (9) that $T - T_p$ is proportional with the input electrical power per unit length (Q/L), thus the axial temperature increases with increasing current and pressure and for same Q/L is independent of the radius of the tube.

Laderman and Byron [11] found the exact solution for the heat equations, and the diffusion equation for the electrons.

They showed that the radial distribution of the electron density differs only slightly from the Bessel profile used here for temperatures at the center of the tube less than 600 K. They also found the temperature at the center of the tube to be a function of the input power per unit length only.

The sources of heat are going to be estimated in two ways.

First by using eq. (8) assuming that the gas temperature is due to the energy transferred from the electrons to the molecular vibrations and subsequent relaxation to ground level. From fig. 1 one obtains

$$q_0 = [(R_1 - R_2)N_0 - R_3 N_3^2 - k_{3c} N_c N_3] E_3, \qquad (10)$$

where Ne is the electron density, E_3 is the vibrational energy of quantum ν_3 , $E_3 = 4.6658 \times 10^{-20}$ J.

Second, using eq. (9) and the input power per unit length estimated from

$$\frac{Q}{L} = I \cdot E = I \cdot N \cdot \frac{E}{N} = I \cdot \frac{p}{kT} \cdot \frac{E}{N}, \qquad (11)$$

where N and p are the total density, and pressure of the gas mixture, E is the axial electric field and I the discharge current.

Lowke et al [12] have solved numerically the Boltzmann equation and derived the transport coefficients for the electrons in the gas mixtures specific to CO_2 lasers. For $j/p = 10^{-3} - 10^{-1}$ A cm^{-2} torr^{-1} typical for CO_2 lasers with wave guide (j is the current density) E/N varies between (2-5) x 10^{-16} V cm^2. In the following we assume E/N = 3 x 10^{-16} V cm^2 thus (11) becomes

$$Q/L\ (\mathrm{W\ m}) \simeq I\ (\mathrm{mA}) \cdot p\ (\mathrm{torr}). \qquad (12)$$

The thermal conductivity of the gas mixture, λ_{mix}, is approximated using a formula given by Mason and Saxena [13]

$$\lambda_{mix} = \sum_{i=1}^{n} \lambda_i \left(1 + \sum_{\substack{k=1 \\ k \neq i}}^{n} G_{ik} \frac{\phi_k}{\phi_i} \right)^{-1}, \qquad (13)$$

where n is the number of gases in the mixture, λ_i and ϕ_i are the thermal conductivity and molar fraction of the i-th component, G_{ik} is a function of the molecular weight of component i and the viscosities of components i and k. For the CO_2 + N_2 + He, and the mixture [3]

$$\lambda_{mix} = \frac{\lambda_{CO_2}}{1 + 0.81 \phi_{N_2}/\phi_{CO_2} + 0.23 \phi_{He}/\phi_{CO_2}} + \frac{\lambda_{N_2}}{1 + 1.4 \phi_{CO_2}/\phi_{N_2} + 0.34 \phi_{He}/\phi_{N_2}} + \frac{\lambda_{He}}{1 + 3.4 \phi_{CO_2}/\phi_{He} + 2.7 \phi_{N_2}/\phi_{He}}, \qquad (14)$$

where λ_{CO_2}, λ_{N_2}, λ_{He} are the conductivities of the pure gases and ϕ_{CO_2}, ϕ_{N_2}, ϕ_{He} are the molar fractions.

The thermal conductivities of the pure gases (in $WK^{-1}m^{-1}$) and their temperature dependence were measured by Booth and Gibbs [14]: $\lambda_{CO_2} = 4.58 \cdot 10^{-5} T^{1.019}$; $\lambda_{N_2} = 3.97 \cdot 10^{-4} T^{0.723}$; $\lambda_{He} = 5.48 \cdot 10^{-3} T^{0.577}$

The thermal conductivity of the wall λ_p, is for Pyrex glass (borosidicate 732) $\lambda_p = 0.172\ T^{0.33}$ [15], for alumina $\lambda_p = 37.7$ [16] and for berillia $\lambda_p = 219.8$.

The temperature dependence of the thermal conductivity of the mixture CO_2 + N_2 and He is shown in fig. 2. Figure 3. presents the thermal conductivity λ_{mix} of CO_2 + He and N_2 + He mixtures as a function of the molar fraction of the He. Due to the high thermal conductivity of He, the conductivity of the mixture is higher the higher the fraction of He and the higher the temperature.

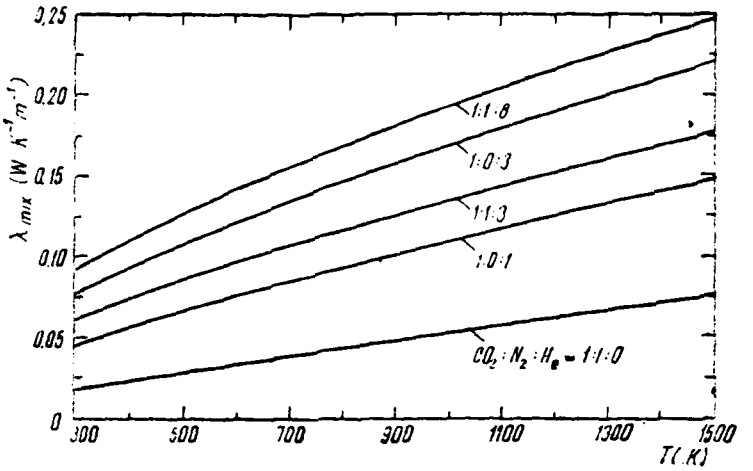

Figure 2. Temperature dependence of the thermal conductivity for some CO_2 + N_2 and He mixtures.

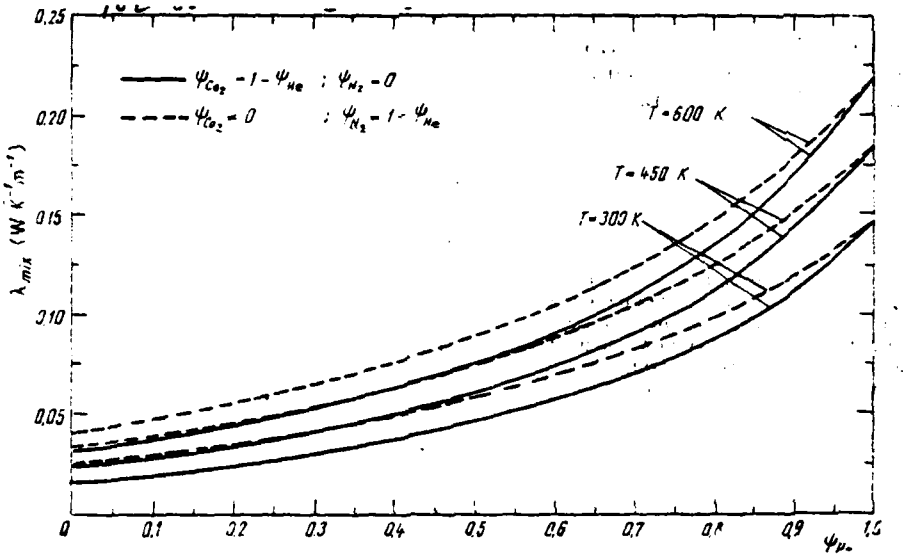

Figure 3. Thermal conductivity of CO_2 and He and N_2 and He mixtures as a function of the molar fraction of He

Due to the temperature dependence of the conductivity of the mixture, the temperature is calculated from equation (8) and (9) by iteration. We assume initially $T = T_p$, and then λ_{mix} and the temperature of the mixture are calculated. Then λ_{mix} is recalculated for the new temperature and the process is repeated. The iteration is continued until the difference between two successive calculated temperatures is less than 1 K.

Figure 4 shows the difference between the temperature at the center of the tube and the wall temperature as a function of the input power per unit length for the $CO_2 : N_2 : He = 1:3:16$ $CO_2 : N_2 : He = 1:1.66:4$ mixtures. The continuous lines are obtained using (9), the dashed lines are due to Laderman and Byron [11] for the same mixtures. The circles are experimental results by the same authors for the 1:3:16 mixture. The agreement between our calculation and the experimental data is excellent.

T - Tp is a strong function of the wall material, as can be seen from figure 5. Thus, the curve a'=4 mm is for Pyrex glass and the curve a' = 1 mm is for all purposes valid for alumina or berillia tubes (or when the temperature gradient in the wall is neglected). For a Pyrex glass tube with a = 1 mm and a' = 4mm and a mixture $CO_2 : N_2 : He = 1:1:3$, the temperature graident in the wall for $T - T_p = 500$ K is over 20% of $T - T_p$.

Figure 6 shows the difference between the temperature at the center of the tube and the wall temperature as a function of the total pressure, for various discharge currents. The continuous lines are calculated from (9), circles are calculated from (8), for the same discharge conditions. The populations in (8) are obtained by solving on the computer the system of equations presented in section 3. The ratio η^*/η^{**} was taken to be 1.45 for I=2 mA, 1.73 for I=5 mA and 1.97 for I=8 mA. The results obtained via these two methods are in very good agreement. In the following the temperature of the gas mixture at the center of the tube is calculated from (9) only, due to the fact that the computer time is much less.

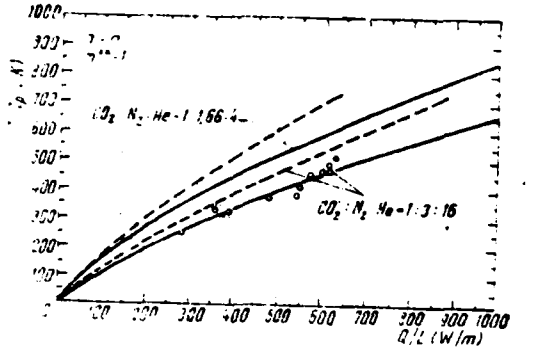

Figure 4. Difference between temperature at the center of the tube and at the wall as a function of input power per unit length for the mixtures CO_2: N_2:He = 1:3:16 and 1:1:66:4.

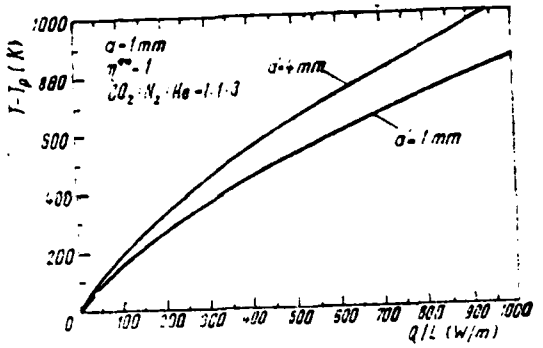

Figure 5: Difference between temperature at the center of the tube and at the wall as a function of input power per unit length with and without temperature gradient in the wall.

Figures 7-9 show the temperature of the gas mixture at the center of the discharge tube for $\eta^{**} = 0{,}15$, as a function of the total pressure, discharge current and respectively the wall temperature (temperature of the cooling agent). Figures 10-11 show the calculated temperature versus the molar fraction of N_2 and He respectively. The temperature is lower the lower the input power (smaller p and I) the lower the temperature of the cooling jacket, the lower the molar fraction of N_2 and the molar fraction of the higher.

Figure 6. Difference between temperature at the center of the tube and at the wall, as a function of total pressure in the tube, for various discharge currents, calculated by the two methods.

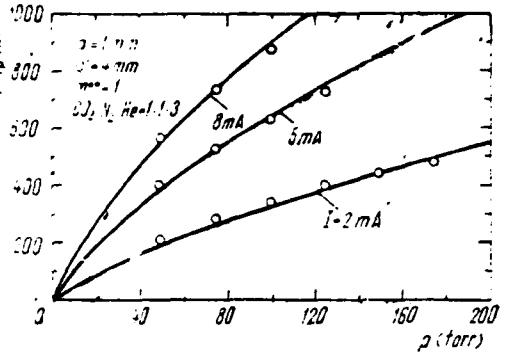

Figure 7. Temperature of the gas mixture at the center of the tube as a function of total pressure, composition of the mixture as parameter (fraction of He).

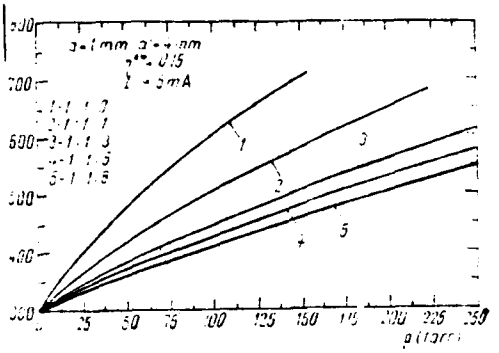

Figure 8. Current dependence of the temperature of the gas mixture at the center of the tube.

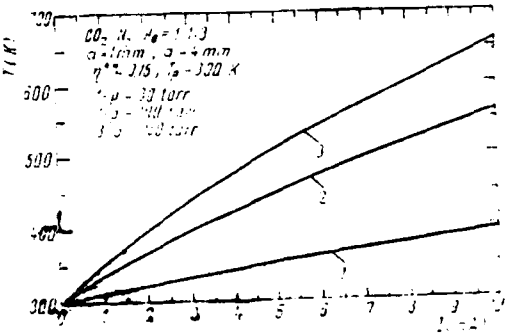

Figure 9. Temperature of gas mixture at the center of the tube as a function of the capillary wall temperature.

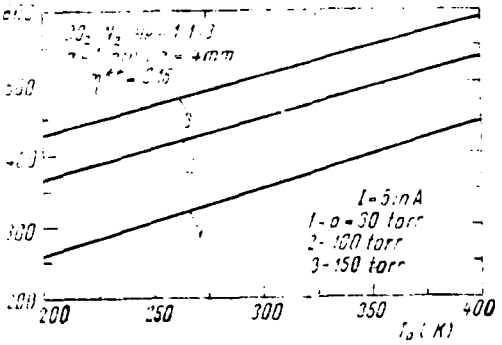

Figure 10 Temperature of the gas mixture at the center of the tube as a function of N_2 content for the mixture $CO_2 : N_2 : He = 1 : f_{N_2} : 3$.

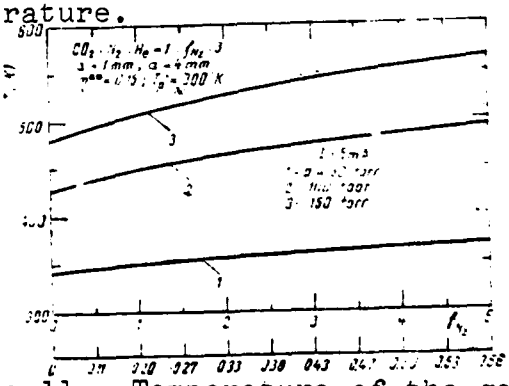

Figure 11. Temperature of the gas mixture at the center of the tube as a function of the content for the mixture $CO_2 : N_2 : He = 1 : f_{N_2} : f_{He}$.

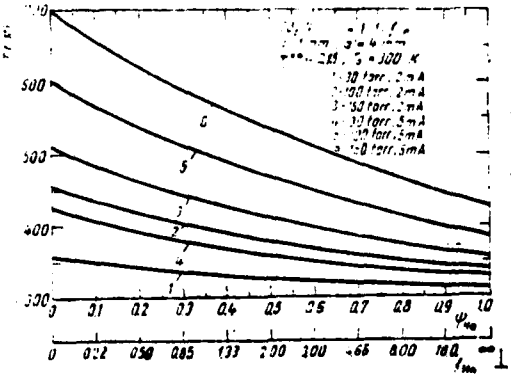

2.2. Electron Density

Experimental studies [10] have proven that the electron density is almost linear in the discharge current, the proportionality constant being a function of the gas mixture. The proportionality constant is estimated using the results in [12], which show that the drift velocity of the electrons, v_D, for E/N in the range (2-5) x 10^{-16} V/cm^2, is in the range (4-8) x 10^6 cm/s and depends only slightly on the gas mixture. The E.N ratio is determined by the necessity to keep the ionization at a high enough rate to balance the loss of charged particles in a self-maintained discharge, and to optimize the efficiency of the vibrational excitation in the laser discharge. Experimental measurements on a laser with waveguide [17] give a ratio E/N of 2.3 x 10^{16} Vcm^2 (from the slope of the voltage-pressure curve). For this value calculations in [12] give $v_D = 4 \cdot 10^6$cm/s . If we substitute the drift velocity in

$$j = N_e v_D e, \tag{15}$$

where N_e is the electron density, and e the electron charge, we obtain $N_e(\text{cm}^{-3}) = 1{,}5 \cdot 10^9\ j(\text{mA/cm}^2)$. The optimum population inversion is in a narrow range of the fractional ionization Ne/N = 10^{-8} - 10^{-7}. As has been previously shown, the electron distribution across the discharge tube is not uniform and thus the current density can not be obtained from the current/area ratio. Assuming the same radial electron distribution as in the previous paragraph (Bessel) and using the integration of this distribution from (6), one obtains:

$$j\,(\text{mA/cm}^2) = 73{,}73\ I(\text{mA})/a^2(\text{mm}^2) \tag{16}$$

and thus $N_e\,(\text{cm}^{-3}) = 1{,}106 \cdot 10^{11}\ I(\text{mA})/a^2(\text{mm}^2)$.

2.3. Rates of Vibrational Excitation

Pumping rates electron molecule for each energy level, R,

are a function of the transverse cross section of vibrational excitation by the electron, σ , and of the electron distribution function, which in turn, is a function of all the important collisional processes.

$$R = \sigma v_D N_e \tag{17}$$

Thus the excitation rates for each vibrational level are different for each gas mixture and for each value of E/N. Moreover in the case of N_2 molecules, the first 8 vibrational levels are excited. The problem is simplified significantly, if an effective rate for the vibrational excitation by electrons of the first vibrational level is defined.

Nighan [19] calculated these rates for N_2 and CO_2 as a function of the average electron energy (which for a Maxwell distribution represents the electron temperature). For average energies larger than 1.5 eV, typical for CO_2 lasers, one obtains $R_1 = 4 \times 10^{-9}$ Ne, $R_2 = 6 \times 10^{-9} N_e$ and $R_3 = 2 \times 10^{-8} N_e$ where R is in sec^{-1} and N_e is in cm^{-3}.

2.4. Rates of Collisional Relaxation

The collisional relaxation rate $k(s^{-1})$ in a CO_2, N_2 and He mixture is obtained from

$$k = k^{CO_2} p_{CO_2} + k^{N_2} p_{N_2} + k^{He} p_{He}, \tag{18}$$

or

$$k = (k^{CO_2}\psi_{CO_2} + k^{N_2}\psi_{N_2} + k^{He}\psi_{He})p, \tag{19}$$

where k^i are the collisional relaxation rates in the pure gases expressed in s^{-1} $torr^{-1}$.

A survey of the experimental measurements of the rates k^i and their temperature dependence, is given in [8], [9]. In calculating population and gain the following values for the col-

lisional relaxation rates are used:

$$k_{32}(\mathrm{cm^3 s^{-1}}) = 4{,}197 \cdot 10^{-14} T^{1/2} \exp\,[10^{-3} T(8{,}84 \cdot 10^{-4} T - 2{,}07)], \tag{20}$$

valid in the range 300-3000K; at 300K, $k_{32} = 13\,623\ \mathrm{s^{-1}\ torr^{-1}}$;

$$k_{21}^{CO_2} = \exp(11{,}32 + 7{,}495 T^{-1/3} - 632{,}14 T^{-2/3} + 2\,239 T^{-1}), \tag{21}$$

valid in the range 250-2500K; at 300K, $k_{21}^{CO_2} = 329\ \mathrm{s^{-1}\ torr^{-1}}$;

$$k_{21}^{N_2} = \exp(-11{,}484 + 507{,}83 T^{-1/3} - 4\,574{,}9 T^{-2/3} + 12\,724 T^{-1}), \tag{22}$$

valid in the range 300-1000K; at 300 K, $k_{21}^{N_2} = 109\ \mathrm{s^{-1}\ torr^{-1}}$;

$$k_{21}^{He} = \exp(24{,}538 - 265{,}48 T^{-1/3} + 763{,}32 T^{-2/3} + 718{,}83 T^{-1}), \tag{23}$$

valid in the range 300 -1000K, at 300K, $k_{21}^{He} = 73\ \mathrm{s^{-1} torr^{-1}}$;

$$k_{12} = k_{21} \exp\,(-\Delta E/kT) = k_{21} \exp(-1382{,}8 T^{-1}); \tag{24}$$

$$k_{10}^{CO_2} = 3{,}09 \cdot 10^9\, T^{-1} \exp\,(-72 T^{-1/3}), \tag{25}$$

valid in the range 300 - 3000K, at 300K, $k_{10}^{CO_2} = 219\ \mathrm{s^{-1} torr^{-1}}$;

$$k_{10}^{N_2} = 4{,}538 \cdot 10^8 T^{-1} \exp\,(-72 T^{-1/3}), \tag{26}$$

valid in the range 300 - 3000K, at 300 K, $k_{10}^{N_2} = 32\ \mathrm{s^{-1}\ torr^{-1}}$; (27)

$$k_{10}^{He} = 4{,}635 \cdot 10^{-8}\ T^{-1} \exp\,(-40{,}63 T^{-1/3}),$$

valid in the range 300-3000K, at 300K, $k_{10}^{He} = 3\,573\ \mathrm{s^{-1}\ torr^{-1}}$; (28)

$$k_{01} = k_{10} \exp\,(-960{,}38 T^{-1}).$$

2.5. Rates of Electron Relaxation

The only levels which relax through electron collisions are 00°1 in CO_2 and v = 1 in N_2.

The relaxation of the CO_2 molecules from the 00°1 level through electron collisions takes place on one of the levels in group 1 and not directly to ground level, as was assumed in [2] - [5]. This rate is [20]: $k_e = 1{,}77 \cdot 10^{-9}\ \mathrm{cm^3\ s^{-1}}$, thus for

$N_e = 3 \cdot 10^{11} cm^{-3}$ typical for a waveguide laser $N_e k_{3e} = 5{,}3 \cdot 10^3 s^{-1}$. This rate compares well with the measurements by Gower and Carswell [21] $(5 \cdot 10^3\ s^{-1})$, and is somewhat smaller than that of Moore et al [1] $(2 \cdot 10^3 s^{-1})$.

The v = 1 level of N_2 is assumed to relax through electron collisions at a rate $k_{3e} = R_3/N_e = 2 \cdot 10^{-8}\ cm^3\ s^{-1}$. This assumption was used by Moore [1] and Gordietz [2]-[4].

2.6. Relaxation rates through diffusion and collisions at the walls.

The relaxation rates through diffusion and collisions at the wall in calculated from [3]

$$k_p = \mu^2 D/a^2 \tag{29}$$

where D is the diffusion coefficient, and μ is the solution of

$$\mu J_1(\mu) = \left(\frac{a\bar{v}}{2D}\right)\left(\frac{1-r}{1+r}\right) J_0(\mu), \tag{30}$$

where $\bar{v}$ is the average velocity, $J_0(\mu)$ and $J_1(\mu)$ are the Bessel functions of the first species of order 0 and 1 respectively, and r is the reflection coefficient of the wall (reflection coefficient = 1 - accomodation coefficient).

For a hollow circular wave guide equation (30) can be simplified by a Taylor series development around μ = 2.405 [7]

$$\mu = 2{,}405 \frac{(1-r)\bar{v}a - 2(1+r)D}{(1-r)\bar{v}a}. \tag{31}$$

The reflection coefficient of the wall was measured by Kovacs et al [22] and is r = 0.78. The average velocity of the CO_2 molecules depends on temperature only $\bar{v}(cm/s) = 2{,}195 \cdot 10^3 \sqrt{T(K)}$

In a CO_2, N_2, He mixture the diffusion coefficient is

obtained from [8]

$$\frac{1}{D} = \sum_i \frac{3N_i\sigma_i}{\bar{v}\alpha} = \sum_i \frac{3p_i\sigma_i}{k\left(\frac{8k}{\pi M}\right)^{1/2}\alpha T^{3/2}}, \tag{32}$$

or

$$\frac{1}{D_i} = \left(\frac{300}{T}\right)^{3/2}\sum_j \frac{p_j}{D_{ij}}, \tag{33}$$

where N_i is the density of species i, σ_i is the collision cross section and α is a constant. For the case of CO_2 and N_2

$$\frac{1}{D_{CO_2}} = \left(\frac{\psi_{CO_2}}{D_{CO_2-CO_2}} + \frac{\psi_{N_2}}{D_{CO_2-N_2}} + \frac{\psi_{He}}{D_{CO_2-He}}\right)p\left(\frac{300}{T}\right)^{3/2}, \tag{34}$$

$$\frac{1}{D_{N_2}} = \left(\frac{\psi_{CO_2}}{D_{N_2-CO_2}} + \frac{\psi_{N_2}}{D_{N_2-N_2}} + \frac{\psi_{He}}{D_{N_2-He}}\right)p\left(\frac{300}{T}\right)^{3/2}. \tag{35}$$

The D_{i-j} constants are those of Gordietz et al [3] at $p = 1$ torr: $D_{CO_2-CO_2} = 51$ cm²/s (Fordietz gives 86 cm²/s, but this was corrected to agree with the value of 0.066 cm^2/s reported by Kovacs et al [22] at 1 atm for CO_2 molecules in the 00°1 state), $D_{CO_2-N_2} = 120$ cm²/s, $D_{CO_2-He} = 500$ cm²/s, $D_{N_2-CO_2} = 130$ cm²/s, $D_{N_2-N_2} = 160$ cm²/s $D_{N_2-He} = 560$ cm²/s.

Thus

$$k_{1p} = k_{2p} = \mu^2_{CO_2} D_{CO_2}/a^2, \tag{36}$$

$$k_{3p} = \mu^2_{N_2} D_{N_2}/a^2. \tag{37}$$

2.7 Fractions of excited molecules on the upper and lower laser levels

The fractions of molecules f_2 and f_1 on the upper and lower laser level are calculated from [23]

$$f(i) = g_i \exp\left(-\frac{i\Delta E}{kT_v}\right)\left[\sum_{i=1}^{\infty} g(i)\exp\left(-\frac{i\Delta E}{kT_v}\right)\right]^{-1}, \tag{38}$$

where f(i) is the fraction of molecules on the i-th vibrational level, expressed for a simple harmonic oscillator; g_1 are the degeneracies, which for the symmetric and asymmetric elongation mode of CO_2 are unity and for the deformation mode of CO_2, CO_2, $g_i = q + 1$; T_v is the vibrational temperature.

In particular for the 00°1 level

$$f_2 = \frac{\exp(-\Delta E_2/kT_{v2})}{\exp(-\Delta E_2/kT_{v2}) \sum_{i=1}^{\infty} \exp\left(-\frac{i\Delta E_2}{kT_{v2}}\right)} = 1 - \exp\left(-\frac{\Delta E_2}{kT_{v2}}\right) = 1 - x_2, \tag{39}$$

where

$$x_2 = \exp\left(-\frac{\Delta E_2}{kT_{v2}}\right) = \frac{N_2 Q_{vib}}{N_t}, \tag{40}$$

Q_{vb} is the vibrational partition function.

Because $N_2/N_t \ll 1$ .is a good approximation. The $f_2 \simeq 1$ modes are characterized by the same vibrational temperature, T_{v1}. The lower laser level relaxes rapidly collisionally to the 01^{10} level, half the level (10°0, 02°0), . Thus the fraction f_1 on the lower level is twice the fraction on the level 01^{10}

$$f_1 = \frac{3x_1^2}{\sum_{i=1}^{\infty} (i+1)x_1^i}, \tag{41}$$

where

$$x_1 = \exp\left(-\frac{\Delta E_1}{kT_{v1}}\right) = \frac{N_1 Q_{vib}}{N_t}. \tag{42}$$

Summing in the denominator

$$f_1 = \frac{3x_1(1-x_1)^2}{3-2x_1}. \tag{43}$$

for $T_{v1} = 300$ K, $x_1 = 0{,}04073$ $f_1 = 0{,}0387$. The function f_1 has a maximum for $x_1 = 0{,}10692$ ($T_{v1} = 1067{,}87$K), , for which $f_1 = 0{,}19641$. At $T_{v1} = 400$ K, $f_1 = 0{,}09$.

2.8. Induced Emission and Absorption

The rate of induced emission in the presence of monochromatic radiation with intensity $I_\nu(\mathrm{W/m^2})$ at the center of the line, is obtained from Einstein's treatment [24]

$$W_{21} = \frac{A_{21}c^2 I_\nu}{8\pi h \nu_0^3} g(0) F_2, \tag{44}$$

where A_{21} is the Einstein coefficient of spontaneous emission ($A_{21} = 0{,}2\ s^{-1}$ for the P(20) line of transition $00^\circ1 \rightarrow (10^\circ0, 02^\circ0)_I$), $g(0)$ is the form function at the center of the line, and $F_2 = N_J/N_2$ is the fraction of molecules on the upper laser level (00°1) which are in the state characterized by the quantum rotational number $J \pm 1$ is obtained from

$$F_2 = \frac{g_J}{Q_{rot}} \exp\left(-\frac{E_J}{kT_r}\right), \tag{45}$$

where $E_J = F(J)hc$ is the energy of the rotational level J with respect to the ground rotational level, and $F(J) \simeq BJ(J+1)$; $Q_{rot} = kT_r/\sigma hcB$ is the rotational partition function, B is the rotation constant of the corresponding vibrations level and σ is the molecular symmetry number (σ=2 for the CO_2 module); T_r the rotational temperature, assumed equal to the kinetic temperature of the gas. For J = 20 and T_r = 400 K, F_2 = 0.063989.

For the CO_2 laser, with wave guide, $g(0) = 2/\nu_c$, where ν_c is the collision frequency, thus (44) becomes

$$W_{21} = 1{,}03 \cdot 10^{13} I_\nu F_2/\nu_c. \tag{46}$$

To calculate the collision frequency for the P(20) line one uses [25]

$$\nu_c = \zeta\left(\frac{300}{T}\right)^{1/2}(\psi_{CO_2} + a_1\psi_{N_2} + a_2\psi_{H_2O})p, \tag{47}$$

where $\zeta = 2{,}248 \cdot 10^7 K^{1/2} s^{-1} torr^{-1}$, $a_1 = 0{,}733$ $a_2 = 0{,}641$.

The rate of induced absorption is correlated to that of induced emission by

$$W_{12} = (g_2/g_1) W_{21} = 9{,}32 \cdot 10^{11} I_\nu F_2 / \nu_c. \tag{48}$$

The net exchange of molecules between the upper and lower laser levels due to induced emission and absorption is

$$W = W_{21} f_2 N_2 - W_{12} f_1 N_1 = W_{21} \left(f_2 N_2 - \frac{g_2}{g_1} f_1 N_1 \right). \tag{49}$$

3. Equation system and its solution

Returning to figure 1 we can write the equation system which characterizes the population dynamics for the four levels of our model

$$\frac{dN_1}{dt} = R_1 N_0 + r(k_{21} N_2 - k_{12} N_1) + s(k_{01} N_0 - k_{10} N_1) - \\ - k_{1p} N_1 + k_{2e} N_e N_2 + W, \tag{50}$$

$$\frac{dN_2}{dt} = R_2 N_0 - k_{2e} N_e N_2 - k_{21} N_2 + k_{12} N_1 + \tag{51}$$

$$+ k_{32} N_0 N_3 - k_{23} N_2 N_3^0 - k_{2p} N_2 - W, \tag{52}$$

$$\frac{dN_3}{dt} = R_3 N_3^0 - k_{3e} N_e N_3 - k_{32} N_0 N_3 + k_{23} N_2 N_3^0 - k_{3p} N_3; \tag{53}$$

$$N_t = N_0 + N_1 + N_2, \\ N_{3t} = N_3^0 + N_3. \tag{54}$$

Coefficient r in (50) takes into account that the collisional relaxation of CO_2 molecules in group 2 (with ν_3 excitation results in exciting more than one quantum of the CO_2 molecule from group 1 (with ν_1 and ν_2 quanta excited). Thus the reactions characterized by the global rates k_{21} and k_{12} are [8]

$$CO_2(00^01) + M \rightarrow CO_2(11^10, 03^10)_I + M + \ldots \tag{55}$$

$$CO_2(00^01) + M \rightarrow CO_2(11^10, 03^10)_{II} + M + \ldots \tag{56}$$

$$CO_2(00^01) + M \rightarrow CO_2(20^00 \ldots 04^00)_{III} + M + 199\ \text{cm}^{-1}, \tag{57}$$

where M can be CO_2, N_2 or He. Reactions (55), (56) are characterized by r = 3/2 and reaction (57) by a coefficient r = 2[5].

Coefficient s in (50) taken into account that the collisional relaxation of molecules from group 1 takes place mostly through reaction [8], [9].

$$CO_2(01^10) + M \rightarrow CO_2(000) + M + 667\ \text{cm}^{-1}. \tag{58}$$

Because the lower laser level has an energy approximately twice that of level 01^10, reaction (58) is equivalent to relaxation of only 1/2 quantum ν_1; thus s= 1/2.

For the system (50)–(54) we have to take into account the radial distribution of the electrons and thus the radial Bessel distribution of N_e, R_1, R_2, R_3, N_1, N_2 and N_3. Integrating these equations across the section (assumed circular) of the discharge tube, at steady state (d/dt = 0) leads to a new system of equations:

$$R_1N_0C_1 + rk_{21}N_2C_1 - rk_{12}N_1C_1 + sk_{01}N_0 - sk_{10}N_1C_1 - k_{1e}N_1C_1 + k_{2e}N_eN_2C_2 + WC_1 = 0, \tag{59}$$

$$R_2N_0C_1 - k_{2e}N_eN_2C_2 - k_{21}N_2C_1 + k_{12}N_1C_1 + k_{32}N_0N_3C_1 - k_{23}N_2N_3^0C_1 - k_{2e}N_2C_1 - WC_1 = 0, \tag{60}$$

$$R_3N_3^0C_1 - k_{3e}N_eN_3C_2 - k_{32}N_0N_3C_1 + k_{23}N_2N_3^0C_1 - k_{3e}N_3C_1 = 0, \tag{61}$$

$$N_e - N_0 - N_1C_1 - N_2C_1, \tag{62}$$

$$N_{3e} - N_3^0 + N_3C_1, \tag{63}$$

where

$$C_1 = \frac{1}{\pi a^2}\int_0^{2\pi} d\varphi \int_0^a r J_0(2{,}405\, r/a)\,dr \simeq 0{,}434, \tag{64}$$

$$C_2 = \frac{1}{\pi a^2}\int_0^{2\pi} d\varphi \int_0^a r J_0^2(2{,}405\, r/a)\,dr \simeq 0{,}270, \tag{65}$$

and N_1, N_2 and N_3 in the new system of equations are the axial densities (peak).

Introducing the notation $k'_{01} = k_{01}/C_1$, $k'_{2e} = k_{2e}C_2/C_1$, $k'_{3e} = k_{3e}C_2/C_1$; $R'_1 = R_1C_1$, $R'_2 = R_2C_1$, $R'_3 = R_3C_1$, $k'_{32} = k_{32}C_1$ and

$$K_1 = R'_3 + k'_{3e}N_e + k_{3p},$$

$$K_2 = R'_2 + k'_{2e}N_e + k_{21} + k_{2p}, \tag{66}$$

$$K_3 = \frac{R'_1 + rk_{12} + sk_{01} + sk_{10} + k_{1p} + W_{12}f_1}{rk_{21} - R'_1 - sk_{01} - k'_{2e}N_e + W_{21}f_2}, \tag{67}$$

$$K_4 = -\frac{R_1 + sk'_{01}}{rk_{21} - R'_1 - sk_{01} + k'_{2e}N_e + W_{21}f_2}, \tag{68}$$

$$K_5 = k'_{32}(R'_2 - k_{12} + K_3W_{21}f_2 - W_{12}f_1 + K_2K_3), \tag{69}$$

$$K_6 = k_{32}(k_{12} - R'_2 - K_3W_{21}f_2 + W_{12}f_1 - K_2K_3) + \tag{70}$$

$$+ k'_{32}(K_4W_{21}f_2 + K_2K_4 - R_2), \tag{71}$$

$$K_7 = -k'_{32}R_3 - k_{32}K_4K_3, \tag{72}$$

$$K_8 = K_4(k_{12} - R'_2 - K_3W_{21}f_2 - W_{12}f_1 - K_2K_3), \tag{73}$$

$$K_9 = k_{32}(R_2 - K_4W_{21}f_2 - K_2K_4), \tag{74}$$

$$K_{10} = K_4(R_2 - K_4W_{21}f_2 - K_2K_4), \tag{75}$$

$$K_{11} = k_{32}(R_3 - K_4K_4), \tag{76}$$

we can determine the population of groups 1, 2 and 3.

$$N_1 = \frac{-(K_6N_t + K_7N_{3t} + K_8) -}{2K_5}$$

$$\frac{-\sqrt{(K_6N_t + K_7N_{3t} + K_8)^2 - 4K_5(K_9N_t^2 + K_{10}N_t + K_{11})}}{2K_5} \tag{77}$$

(we choose the solution with minus before the square root, because the one with plus gives a density of molecules in group 1 larger than the total density of CO_2 molecules)

$$N_2 = K_3N_1 + K_4N_t, \tag{78}$$

$$N_3 = (k_{12} - R'_2 - W_{12}f_1)N_1/K_1 - (K_2 + W_{21}f_2)N_2/K_1 + \tag{79}$$

$$+ (R_3N_{3t} + R_2N_t)/K_1,$$

and the number of CO_2 and N_2 molecules in the ground state using equations (62) and (63)

Thus the solution of the system of equations which characterize a CO_2 laser with wave guide allow the determination of the population inversion and the population of the laser levels.

The small signal gain at the center of a line in the P branch is calculated from these populations (with $I_s = 0$, and $W_{12} = W_{21} = 0$) in [24]

$$\alpha_0(P) = K_c F(v, J) J \frac{\nu_J}{\nu_0} \left\{ \frac{N_2 B_2}{N_1 B_1} \exp\left[-J(J-1) \frac{\theta_2}{T_r} \right] - \exp\left[-J(J-1) \frac{\theta_1}{T_r} \right] \right\},$$

where

$$K_c = \frac{16\pi^3 \sigma \nu_0}{3k T_r \nu_c} \quad R_{v_1}^{v_2} = N_1 B_1, \tag{81}$$

where $R_{v_1}^{v_2} = 4{,}01 \cdot 10^{-2} D$ is the matrix element of the dipole moment for vibrational transitions, $B_1 = 0{,}39018\ \text{cm}^{-1}$, $B_2 = 0{,}38714\ \text{cm}^{-1}$, $\nu_0 = 2{,}880881 \cdot 10^{13}\text{Hz}$ is the central frequency of the band, $F(v, J) = 1 + 0{,}0009J - 0{,}00006J^2$ is the coefficient of interaction vibration rotation, $\nu_J = 2{,}830622 \cdot 10^{13}\text{Hz}$ is the frequency of line P(20), and $\theta = hcB/k$ is the rotational temperature [26] - [28]. Introducing these constants in (80) and (81) for line P(20) of transition 00°1 - $(10°0, 02°0)_I$ we obtain

$$\alpha\left(\frac{dB}{m}\right) = \frac{3{,}622 \cdot 10^{-5}}{\nu_c T} \left[N_2 f_2 \exp(-211{,}7/T) - 1{,}0078 N_1 f_1 \exp(-235{,}8/T) \right] \tag{82}$$

In the exact calculation of the small signal gain one has to take into account the losses in the wave guide. The losses in the propagation mode EH_{11} in the cylindric dual wave guide is given by [29]

$$\alpha_{11} = \left(\frac{u_{11}}{2\pi} \right)^2 \frac{\lambda^2}{a^3} \operatorname{Re}(\nu_a), \tag{83}$$

where $u_{11} = 2,405$ is the first root of equation $J_0(u_{nm}) = 0$, $\lambda = 10,59\ \mu m$ is the wavelength of the radiation propagating through the waveguide and $\nu_n = (\nu^2 + 1)/(2\sqrt{\nu^2 - 1})$, , where ν is the complex index of the wall material ($\nu = 1.910 + 0.077$ for Pyrex glass [30]), thus $\mathrm{Re}(\nu_n) = 1,426$. Under these conditions $\alpha_{11}(dB/m) = 0,105/a^3(mm^3)$

4. Results

Populations of the laser levels, small signal gain and saturation intensity were calculated for various regimes of the CO_2 laser with wave guide. Most of the calculations were done for the mixture $CO_2 : N_2 : He = 1 : 1 : 3$, characteristic for lasers with gas circulation [31], but other mixtures were tested.

Figure 12 shows the variation of the population N_1 and N_2 as a function of the discharge current for three different pressures, for a 1 mm diameter waveguide. For 100 and 150 torr pressure, the population inversion is maintained over the whole range, for 30 torr the population inversion occurs only for currents smaller than 5 mA.

The pressure dependence of N_2/N_1 for various discharge currents is shown in figure 13.

For a 1 mm capillary and $CO_2 : N_2 : He = 1 : 1 : 3$, the maximum of the N_2/N_1 ratio occurs in the pressure range 100 to 150 torr.

To verify our model the small signal gain was calculated for the experimental conditions used by Abrams and Bridges [32], this comparison is presented in figure 14. The agreement is very good as far as the absolute value of the gain is concerned, the experimental curves are shifted toward higher pressures though. This shift can be explained by the use of berillia

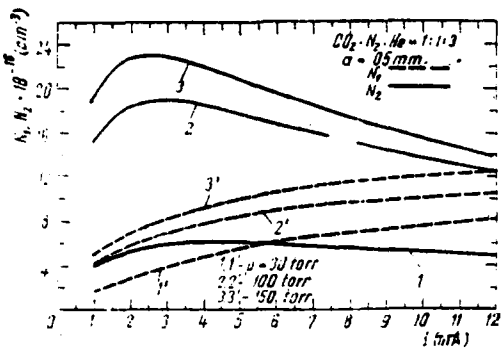

Figure 12. Absolute populations of groups 1 and 2 as a function of the discharge current in a 1 mm capillary.

capillaries in [32] for which the cooling is more efficient and by relaxation rates at the wall different than those used in calculation (for Pyrex glass).

Figures 15 and 16 present the small signal gain as a function of pressure (gas mixture as parameter) and the radius of the wave guide respectively. In figure 15 the gain was calculated for mixtures in which the fraction of He is modified. If for the 1:1:0 mixture the gain decreases monotonously and rapidly with pressure, the mixtures containing He show a maximu. The agreement between experimental measurements of the gain for a laser with a = 1 mm, $I = 8$ mA and $CO_2 : N_2 : He = 1:1:3$ [17] and our calculations is very good. From figure 16 in which the dashed lines represent the calculated gain when neglecting losses in the waveguide, and the continuous one which takes losses into account, we concluded that the optimum diameter for the capillaries is in the range 1-1.5 mm and that losses are important only for diameters smaller than 1.5 mm.

Aside from calculating populations and gain the proposed model can be used to calculate the saturation intensity (saturation parameter). Assuming that in waveguide lasers the line widens homogeneously with pressure, the saturation intensity is determined as the value of intensity for which the small signal gain decreases to half.

Figure 17 shows the pressure dependence of the saturation

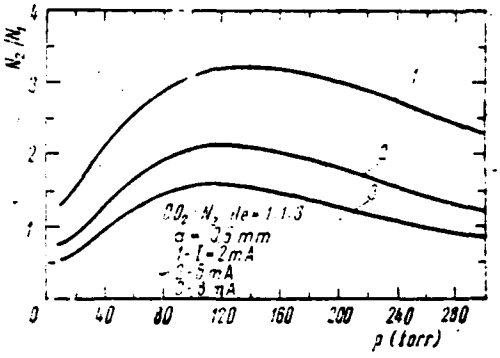

Figure 13. Population ratio for groups 1 and 2 as a function of total pressure (a = 0.5 mm).

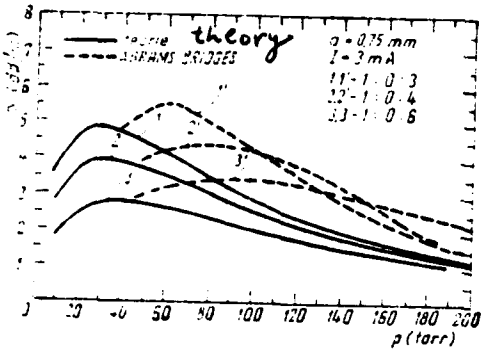

Figure 14. Comparison between calculations of gain and experimental measurements of Abrams and Bridges [32] for the same discharge conditions.

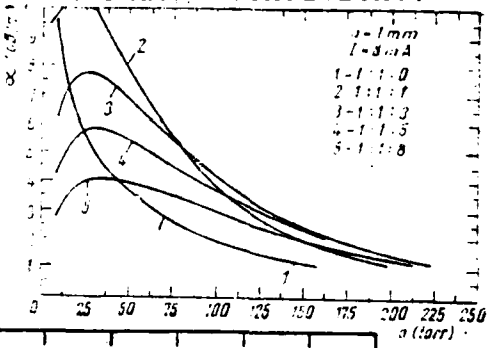

Figure 15. Small signal gain as a function of total pressure in a tube of 2 mm diameter.

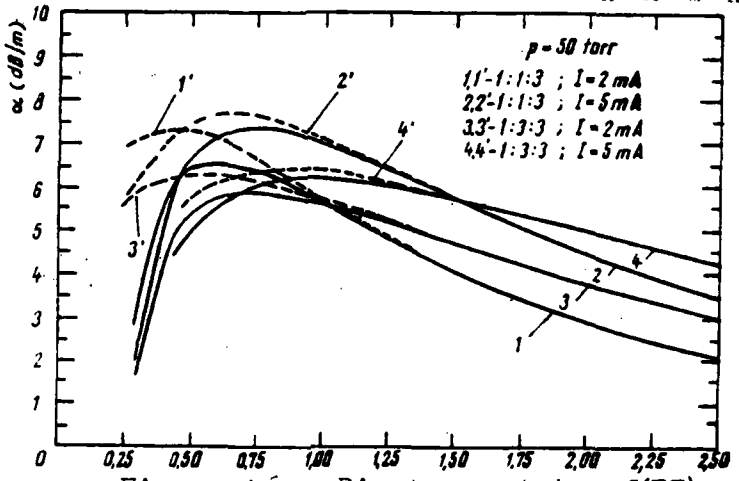

Figure 16. Discharge tube radius dependence of the small signal gain for various mixtures and discharge currents.

intensity for various discharge currents. Saturation intensity increases with pressure- which is also shown by simpler models. The large values of parameter I_s for waveguide lasers can be explained by the large pressures used in these lasers, and because the process of diffusion and relaxation at the wall is more efficient than for conventional lasers (low pressures).

The dependence of the current on saturation intensity for a waveguide 2 mm in diameter is shown in Figure 18. Agreement with the simpler models, which lead to linear increases in the parameters of saturation with current, is likewise good.

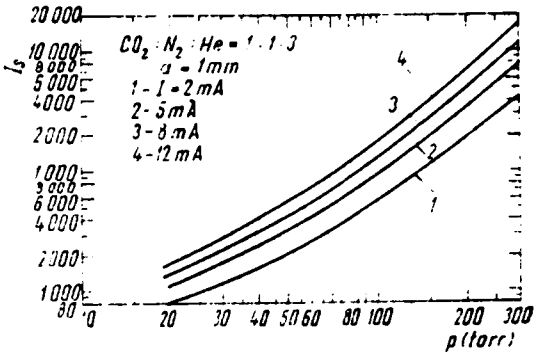

Figure 17. Pressure dependence of the saturation intensity, discharge current as a parameter.

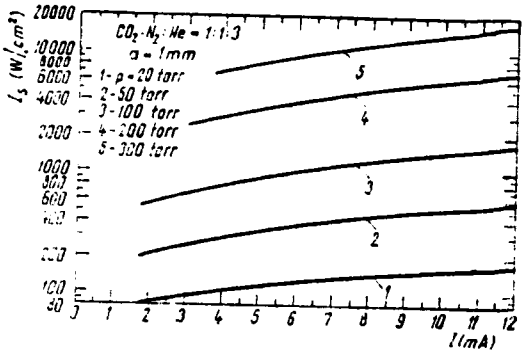

Figure 18. Discharge current dependence of the saturation intensity for a 2 mm tube.

5. Conclusions

A four level system is used to model the physical processes and equations characterizing the CO_2 lasers with waveguide. The system of equation is solved by computer. It allows to determine the dependence of important parameters such as: kinetic temperature, population of laser levels, small signal gain, saturation intensity,as a function of: discharge current, total pressure, gas mixture etc. The agreement between calculations and experiment is satisfactory.

These calculations can be used to optimize the functioning of CO_2 lasers with waveguide according to their use (small size, efficient cooling, high oscillation band). Though the model is applied to waveguide lasers it can be extended to other types of CO_2 lasers.

Referenees

1. C. B. Moore, R. E. Wood, B. L. Hu, J. T. Yardley, J. Chem. Phys., **46**, *11*, 1222 (1967).
2. B. F. Gordietz, N. N. Sobolev, V. V. Sokovikov, L. A. Shelepin, Phys. Lett., **25A**, *2*, 173 (1967).
3. B. F. Gordietz, N. N. Sobolev, L. A. Shelepin, J.E.T.F., **53**, *5*, 1822 (1967).
4. B. F. Gordietz, N. N. Sobolev, V. V. Sokovikov, L. A. Shelepin, IEEE J. Quant. Electr., **QE—4**, *11*, 796 (1968).
5. S. C. Cohen, IEEE J. Quant. Electr., **QE—12**, *4*, 237 (1976).
6. H. Shirahata, T. Fujioka, J. Appl. Phys., **46**, *6*, 2627 (1975).
7. H. Shirahata, T. Fujioka, J. Appl. Phys., **47**, *6*, 2152 (1976).
8. D. C. Dumitraș, Stud. cerc. fiz., **28**, *4*, 369 (1976).
9. D. C. Dumitraș, Stud. cerc. fiz., **28**, *7*, 673 (1976).
10. M. Z. Novgorodov, N. N. Sobolev, *The properties of low temperature molecular plasma*. Eleventh International Conference on Phenomena in Ionized Gases, Prague, September 10—14, 1973.
11. A. J. Laderman, S. R. Byron, J. Appl. Phys., **42**, *8*, 3138 (1971).
12. J. J. Lowke, A. V. Phelps, B. W. Irwin, J. Appl. Phys., **44**, *10*, 4664 (1973).
13. E. A. Mason, S. C. Saxena, Phys. Fluids, **1**, *5*, 361 (1958).
14. D. J. Booth, W. E. K. Gibbs, Report 413, *Defence Standards Laboratories*, Maribyrong, Victoria, Australia, November 1970.
15. Catalog *Verrerie de laboratoire*, Sovirel, 1973, p. VIII.
16. R. A. Crane, *Parameter measurements on small CO_2 lasers*, in *Developments in Laser Technology Seminar Proceedings*, Rochester, 17—18 November, 1969.
17. D. C. Dumitraș, N. Comaniciu, Rev. Roum. Phys., **23**, —, (1978).
18. W. L. Nighan, *Progress in high pressure electric lasers*, Eleventh International Conference on Phenomena in Ionized Gases, Prague, September 10—14, 1973.
19. W. L. Nighan, Phys. Rev. A, **2**, 5, 1989 (1970).
20. W. A. Rosser, Jr., E. Hoag, E. T. Gerry, J. Chem. Phys., **57**, *10*, 4153 (1972).
21. M. C. Gower, A. I. Carswell, Appl. Phys. Lett., **22**, *7*, 321 (1973).
22. M. Kovacs, D. R. Rao, A. Javan, J. Chem. Phys., **48**, *7*, 3339 (1968).
23. M. C. Fowler, J. Appl. Phys., **43**, *8*, 3480 (1972).
24. D. C. Dumitraș, Stud. cerc. fiz., **29**, *2*, 133 (1977).
25. D. C. Dumitraș, Stud. cerc. fiz., **28**, *10*, 967 (1976).
26. E. Arié, N. Lacome, C. Rossetti, Can. J. Phys., **50**, *16*, 1800 (1972).
27. T. J. Bridges, T. Y. Chang, Phys. Rev. Lett., **22**, *6*, 811 (1969).
28. K. M. Baird, H. D. Riccius, K. J. Siemsen, Opt. Commun., **6**, *2*, 91 (1972).
29. D. C. Dumitraș, Stud. cerc. fiz., **30**, *2*, 137(1978).
30. J. J. Degnan, D. R. Hall, IEEE J. Quant. Electr., **QE—9**, *9*, 901 (1973).
31. D. C. Dumitraș, N. A. Shubina, E. M. Kudriavtsev, N. N. Sobolev, Rev. Roum. Phys., **20**, *9*, 1001 (1975).
32. R. L. Abrams, W. B. Bridges, IEEE J. Quant. Electr., **QE—9**, *9*, 940 (1973).